Acta Neuropathologica Communications

RESEARCH

Open Access

Glioneuronal tumors *PATZ1*-fused: clinico-molecular and DNA methylation signatures for a variety of morphological and radiological profiles

Arnault Tauziède-Espariat[1,2,3,21*], Volodia Dangouloff-Ros[3,4,5], Philipp Sievers[6,7], Mathilde Duchesne[8], Aurore Siegfried[9,10,11], Yvan Nicaise[9,10], Nathalie Boddaert[3,4,5], Lauren Hasty[1], Alice Métais[1,2,3], Carine Ngo[12], François le Loarer[13,14,15], Corinne Bouvier[16], Alix Fontaine[17,18], Audrey Rousseau[17,18], Florent Marguet[19], Kévin Beccaria[3,20], Thomas Blauwblomme[3,20], Emmanuelle Uro-Coste[9,10,11], Pascale Varlet[1,2,3] and On behalf of the RENOCLIP-LOC

Abstract

The neuroepithelial tumor, *PATZ1*-fused (NET-*PATZ1*), has been recently isolated as a distinct methylation class by DNA-methylation profiling and is characterized by recurrent *PATZ1* fusions, in association with the *EWSR1* or *MN1* genes and a chromosome 22 chromothripsis. The clinical phenotype is mainly pediatric and features circumscribed supratentorial tumors. However, the histopathology is vastly heterogeneous (glial, glioneuronal, sarcomatous, multiphenotypic) and a cell of origin has not yet been identified, explaining the previsionary imprecise terminology of "NET". Moreover, extra-central nervous system (CNS) sarcomas also harboring the *EWSR1::PATZ1* fusion have been reported and added to the current World Health Organization (WHO) Classification of Soft Tissue and Bone Tumors, in the chapter on undifferentiated small round cell sarcomas. However, their relationship to their CNS counterparts has not yet been studied. Herein, we analyzed a cohort of twelve CNS tumors with *PATZ1* fusions in terms of clinical presentation, radiology, histopathology, immunohistochemistry, ultrastructure and DNA-methylation profiling and compared them to five extra-CNS sarcomas-*PATZ1*. Based on the reported *GATA2* overexpression in NET-*PATZ1*, we also studied the potential interest of GATA2 immunoexpression as a diagnostic tool. We confirmed their distinct molecular characteristics and clinical phenotype but evidenced a morphological intratumoral heterogeneity with three recurrent morphological patterns (oligodendroglial-like, pleomorphic xanthoastrocytoma-like and spindle cells). Despite the unusual spindle and proliferative component in a CD34 + glioneuronal tumor (using electronic microscopy), these tumors present a favorable prognosis. Their histopathological features were all clearly distinct from their soft tissue counterparts. GATA2 immunostaining is highly specific for CNS tumors *PATZ1*-fused, but its sensitivity is perfectible and further studies are needed to confirm its use as a diagnostic tool. To conclude, our work highlights that CNS tumors, *PATZ1*-fused seem to represent a novel pediatric glioneuronal

*Correspondence:
Arnault Tauziède-Espariat
a.tauziede-espariat@ghu-paris.fr

Full list of author information is available at the end of the article

tumor type exhibiting a polymorphous morphology and provides new support for its addition as a provisional emerging pediatric circumscribed glioneuronal tumor type, low grade.

Keywords Glioneuronal tumor, EWSR1::PATZ1, MN1::PATZ1, DNA-methylation

Introduction

Over the last few years, DNA-methylation analysis has particularly improved the understanding and the histo-molecular deciphering of CNS tumors, particularly for pediatric and rare tumor types. Most of these methylation classes (MC) are integrated into the latest version of the WHO CNS tumor classification when they represent a unified clinicopathological and molecular tumor type. Recently, a novel MC has been described, characterized by recurrent *PATZ1* fusions (with *MN1* or *EWSR1* genes) and frequent chromosome 22 chromothripsis. To date, 79 cases have been referenced in the literature, but no consensual pathological profile has been drawn, and the temporary name of "neuroepithelial tumor, *PATZ1*-fused" (NET-*PATZ1*) has been used. Indeed, they mainly concern children with circumscribed supratentorial tumors, and feature a wide variety of morphologies (with glioma-, astroblastoma-, ependymoma-, glioneuronal-, and even sarcoma-like features) and a multiphenotypic immunoprofile. Genetic analyses have evidenced an overexpression of NET-*PATZ1* genes, which are known to be implicated in neurogenesis as *GATA2*, *PAX2* and *IGF2* [1]. Moreover, *PATZ1* fusions have also been reported in soft tissue sarcomas and renal cell carcinomas with sarcomatoid features, and the burden of these tumors as compared with their CNS counterparts has not been established [2, 3]. In the present study, we analyzed the clinical, radiological, histopathological, and molecular/epigenetic data from a cohort of CNS tumors with *PATZ1* fusions to better characterize them and compare them with their soft tissue counterparts. We also studied the sensitivity/specificity of GATA2 immunohistochemistry in the diagnosis of CNS tumors with *PATZ1* fusions and their main histopathological differential diagnoses.

Materials and methods

Study design, patients, data collection

This study included patients diagnosed with CNS tumors having *MN1::PATZ1* and *EWSR1::PATZ1* fusions, determined by RNA sequencing analyses (whole exome sequencing or RNA sequeencing analyses with a panel including *MN1* and *EWSR1* genes). Epidemiological data (sex and age at diagnosis) and tumor- and treatment-related data (location of tumor and extension, extent of resection, relapses and complementary treatments) were retrospectively analyzed. The extent of the initial resection was assessed by magnetic resonance imaging (MRI), performed after surgery. All the patients' parents or legal guardians signed informed consent forms before treatment began. Two cases were previously reported in [4] and [5]. Samples from five sarcomas, *PATZ1*-fused were also included to perform histopathological, immunohistochemical, epigenetic and ultrastructural analyses.

Central radiological review

The central radiological review was performed by two neuroradiologists (NB and VDR). Patients underwent preoperative computerized tomography (CT) and magnetic resonance imaging (MRI) and the following features were analyzed: location, tumor size, density on CT (when available), signal on T1-weighted and T2-weighted images, low signal areas on susceptibility-weighted imaging, apparent diffusion coefficient (ADC), enhancement, presence of cysts, necrosis, and tumoral blood flow on arterial spin labeling (ASL).

Central histopathological review and immunohistochemistry

The central pathology review was performed conjointly by two neuropathologists (ATE and PV), and sarcomas by soft tissue pathologists (CN, FLL and CB). All the slides were reviewed and one representative paraffin block was selected for each case for additional techniques. Unstained 3-µm-thick slides of formalin-fixed, paraffin-embedded tissues were obtained and submitted for immunostaining. The following primary antibodies were used: Glial Fibrillary Acidic Protein (GFAP) (1:200, clone 6F2, Dako, Glostrup, Denmark), OLIG2 (1:500, clone OLIG2, Sigma-Aldrich, Saint-Louis, USA), neurofilament (1:100, clone NF70, Dako, Glostrup, Denmark), NeuN (1:1000, clone A60, Sigma-Aldrich, Saint-Louis, USA), synaptophysin (1:150, clone Synap, Dako, Glostrup, Denmark), chromogranin A (1:200, clone LK2 H10, Diagnostic Biosystem, Pleasanton, USA), CD34 (1:40, clone Qbend10, Dako, Glostrup, Denmark), EMA (1:200, clone GM008, Dako, Glostrup, Denmark), CK18 (1:200, clone 6F2, Dako, Glostrup, Denmark), Cytokeratins AE1/AE3 (1:800, clone AE1/AE3, Dako, Glostrup, Denmark), alpha-smooth muscle actin (1:6000, clone S100, Dako, Glostrup, Denmark), desmin (1:200, clone D33, Dako, Glostrup, Denmark), myogenin (prediluted, clone FD5, Dako, Glostrup, Denmark), S100 (1:200, clone 6F2, Dako, Glostrup, Denmark), SOX10 (1:200, clone IHC010, Diagomics, Blagnac, France), GATA2 (1:50, polyclonal, Sigma-Aldrich, Saint-Louis, USA), H3K27me3 (1:2500, polyclonal, Diagenode, Liege, Belgium), CD99 (1:10, clone 12E7, Dako, Glostrup, Denmark), INI1 (BAF47) (1:50, clone 25/BAF 47, BD Biosciences, Franklin Lakes,

USA) and Ki-67 (1:200, clone MIB-1, Dako, Glostrup, Denmark). Reticulin staining was performed using the Reticulin silver plating kit according to Gordon & Sweets (Merck Millipore, Guyancourt, France). External positive and negative controls were used for all antibodies and staining. All the slides were digitalized and the proliferative index of each tumor was calculated automatically by an artificial intelligence software (percentage calculated on 2000 cells).

Next-generation sequencing (NGS)

Next-generation sequencing (NGS) was also performed according to the Illumina NextSeq 500 protocol (Illumina, San Digeo, CA, USA). We employed a custom NGS panel known as DRAGON (Detection of Relevant Alterations in Genes involved in Oncogenetics by NGS), commercially available as SureSelect CD Curie CGP by Agilent. This panel encompasses 571 oncology-related genes, serving diagnostic, prognostic, therapeutic, and predisposition purposes. It covers nucleotide sequences (variants) and copy number alterations (deletions and focal amplifications). Library preparation involved using 50 ng of DNA extracted from frozen tumors with the Agilent SureSelect XT-HS preparation kit, following the manufacturer's protocol. In addition to the 571 genes, the panel incorporates genome-wide probes, offering a copy number profile with an average resolution of one probe every 200 Kb. This allows for a comprehensive copy number profile across all chromosomes. Variant calling was performed using Varscan2 (v2.4.3), while copy number profiles for each tumor were estimated using a combination of in-house R scripts and the facets package (v0.6.0). We used a sex-specific unmatched-germline control sequenced with the same panel for normalization.

DNA methylation profiling

Tissue samples (FFPE or freshly frozen if available), from which 500 ng of DNA was extracted, were analyzed. DNA was extracted using the QIAamp® DNA Tissue kit or QIAamp® DNA FFPE Tissue Kit (Qiagen, Hilden, Germany) for FFPE samples. DNA from FFPE samples was restored using the Infinium HD FFPE Restore Kit (Illumina, San Diego, California, USA). Bisulfite conversion was performed using the Zymo EZ DNA methylation Kit (Zymo Research, Irvine, California, USA). Standard quality controls confirmed the DNA quality/quantity and bisulfite conversion. DNA was then processed using either Illumina Infinium Methylation EPIC or HumanMethylation450 BeadChip (Illumina, San Diego, California, USA) arrays according to the manufacturer's instructions. The iScan control software was used to generate raw data files in.idat format, that were analyzed using GenomeStudio software version v2011 and checked for quality measures in accordance with the manufacturer's instructions. To complement these raw data and as a reference, 406 samples were added from Capper et al. which contained different methylation classes corresponding to each DKFZ v11b4 classification (updated with brain classifier version 12.8) and Bethesda (v2.0). Affiliation predictions for CNS tumor classes were obtained from a DNA methylation-based classification of CNS tumors from DKFZ (Deutsches Krebsforschungszentrum—German Cancer Research Center) based on a random forest algorithm available on the web platform www.molecularneuropathology.org. Version v12.8 of the algorithm was used for the present study. The output of this classifier is a score (calibrated score, CS) indicating the resemblance to the reference CNS tumor class in the algorithm. We chose a dimension reduction technique for data visualization: the t-SNE algorithm (t-distributed stochastic neighbor embedding). This non-linear method permits the visualization of data in the form of scatter plots and is well suited for the analysis of raw methylation data. Distinct samples from the same tumor type will usually lead to compact clusters. However, there is no distance threshold that can serve to determine if one sample of interest belongs to one particular cluster; we thus consider that a sample belongs to one class of reference if it overlaps the corresponding cluster or falls within close vicinity. This method is frequently used in cancer research and to study DNA methylation profiling data in CNS tumors. It was used in the original paper on the classification of central nervous system tumors based on DNA methylation profiles by Capper et al. (15). Parameters used in this study are the same as those from the DKFZ. Data from EPIC and 450k methylation array were analyzed using R (v4.0.4). The minfi package was used to load the idat file and was preprocessed using the function "preprocessIllumina" with dye bias correction and background correction. We removed probes located on sex chromosomes, not uniquely mapped to the human reference genome (hg19), probes containing single nucleotide polymorphisms and probes that are not present in both the EPIC and 450k methylation array. A batch effect correction was effectuated with the "removeBatchEffect" function from the limma package, to remove any difference between the FFPE and frozen samples. The probes were sorted by standard deviation and the 10,000 most variable probes were kept for the clustering analysis. These probes were used to calculate the 1-variance weighted Pearson correlation between samples. The distance matrix was used as input for the t-SNE from the Rtsne package, with the following non-default parameters: theta = 0, pca = F, max_iter = 1000 and perplexity = 10. The ggplot2 package was used for data visualization.

Ultrastructural analyses

A representative section was first selected for each case from FFPE tissues stained with Hemalun Phloxin Saffron. Next, tissues were deparaffinized and fixed one hour in glutaraldehyde. After the dehydration process, the tissues were embedded in Epon. Semi-thin Section (1-µm-thick slides) were stained with toluidine blue. Ultrathin Section (90 nm) were stained with lead citrate and uranyl acetate, then observed under an electronic microscope (JEOL JEM 1400 Flash). The analyses were performed in the Pathology Department of Limoges University Hospital by one neuropathologist (MD).

Results

CNS tumors, PATZ1-fused are mainly pediatric supratentorial neoplasms associated with a good prognosis

Relevant clinical data are summarized in Table 1. The age at diagnosis ranged from 0 to 53 years of age, and concerned mainly children (median age of 15 years). The female-to-male ratio was 1. Only six tumors were centrally reviewed in this study by radiology. Five tumors had a hemispheric location (three parietal and two temporal), while the last case was located, in continuity, in the fourth and third ventricle (case #8). The patients underwent a total tumor resection ($n = 10$) or subtotal resection (patients #8 and #11) and three received adjuvant therapy. The outcome was relatively favorable with 5/12 patients presenting in situ recurrences (among them, two being subtotally resected), with a median progression-free survival of 91 months (ranging from 4 to 144 months). All patients were alive at the end of follow-up, with a median overall survival (OS) of 65 months (ranging from 13 to 180 months).

CNS tumors, PATZ1-fused present intratumoral heterogeneity but recurrent radiological and histopathological features

Imaging phenotypes varied among patients with available MRI (Fig. 1). All had well-defined borders without infiltration into the surrounding brain. The tumors involved the cortex and subcortical white matter, as well as the basal ganglia for the largest ones (patients #1 and #7). Large cysts were seen in 4/6 of them. The tumors had intense contrast enhancement in 4/6 cases, the others presented mild contrast enhancement. All displayed intermediate to low signal on T2-weighted images. When available (two cases for each characteristic), tumors were hyperdense on CT (one case with calcifications), and had restricted diffusion and low cerebral blood flow on perfusion MRI, using arterial spin labeling.

Histopathologically, all tumors were highly polymorphous with different morphological patterns (see supplementary Table 1 for details): 1/ a glial component with round oligodendroglial-like clear cells, separated by a dense vascularization composed of branching vessels harboring a hyaline wall without microvascular proliferation (11/12 samples) (Fig. 2A-C), 2/ a glial pattern with multinucleated cells, without xanthomatous changes (10/12 samples) (Fig. 2D-F), and 3/ spindle cell component (4/12 samples) (Fig. 2G-I). These patterns were variably associated within the same tumor (three patterns in three tumors, two patterns in seven samples), but in two tumors, only one pattern (spindle cell component) was present (Fig. 2M). Although these patterns were not clearly correlated with the genotype, the presence of the spindle cell component was observed in CNS tumors with a *EWSR1::PATZ1* fusion.

The tumors were mostly well-circumscribed from the brain parenchyma (8/12 samples), whereas the remaining cases infiltrated the tumor periphery. Five tumors presented some perivascuslar pseudorosette structures without EMA immunoposivity, and were mostly associated

Table 1 Main clinical and genetic findings of the cohort

Case number	Location	Age (years-old)	Sex	Treatments	Recurrence	PFS (months)	Death	OS (months)	Transcript fusion
1	Right lateral ventricle	3	F	TR	1, in situ	139	0	144	*MN1::PATZ1*
2	Right parietal lobe	2	F	TR, RT	0	66	0	66	*MN1::PATZ1*
3	Left parietal lobe	14	M	TR	0	25	0	25	*EWSR1::PATZ1*
4	Right occipital lobe	53	M	TR	1, in situ	91	0	149	*EWSR1::PATZ1*
5	Right parietal lobe	13	F	TR	1, in situ	144	0	180	*EWSR1::PATZ1*
6	Left parietal lobe	19	M	TR	0	14	0	14	*EWSR1::PATZ1*
7	Right temporal	13	M	TR, RT	0	96	0	96	*EWSR1::PATZ1*
8	Pineal	0	M	STR, CT	1, in situ	4	0	15	*MN1::PATZ1*
9	Frontal lobe	47	M	TR	0	13	0	13	*MN1::PATZ1*
10	Left occipital lobe	16	F	TR	0	64	0	64	*EWSR1::PATZ1*
11	Right lateral ventricle	18	F	STR	1, in situ	5	0	20	*MN1::PATZ1*
12	Left frontal lobe	39	F	TR	0	116	0	116	*EWSR1::PATZ1*

CT: chemotherapy; F: female; M: male; RT: radiation therapy; STR: subtotal resection; TR: total resection

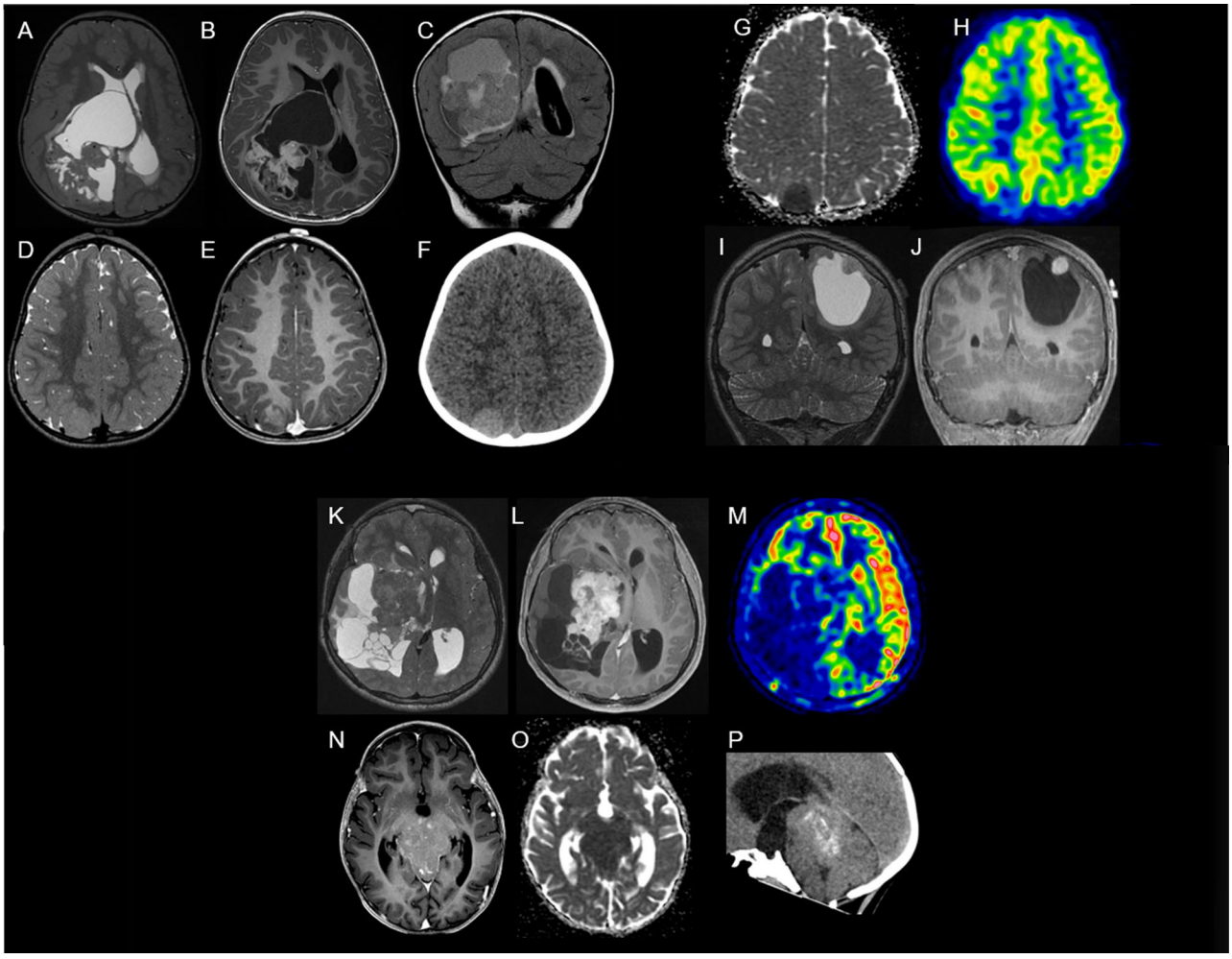

Fig. 1 Imaging features of neuroepithelial tumors, *PATZ1*-fused. **A-C** Imaging of patient #1 on axial T2-weighted (**A**), post-contrast T1-weighted (**B**) and coronal FLAIR (**C**) images, showing a large heterogeneous right intraventricular mass with cystic content and contrast enhancement. **D-H** Imaging of patient #2 on axial T2-weighted (**D**), post-contrast T1-weighted (**E**), unenhanced CT (**F**), apparent diffusion coefficient map (**G**) and cerebral blood flow map (**H**) images, showing a right parietal mass with solid content, partial contrast enhancement, high density, diffusion restriction and low tumoral blood flow. **I-J** Imaging of patient #3 on coronal T2-weighted (**I**) and post-contrast T1-weighted (**J**) images, showing a left parietal cortical mass with a large cyst and a small enhancing nodule. **K-M** Imaging of patient #7 on axial T2-weighted (**K**), post-contrast T1-weighted (**L**) and cerebral blood flow map (**M**) images, showing a large heterogeneous right temporal mass involving the basal ganglia, with cystic content, contrast enhancement and low tumoral blood flow. **N-P** Imaging of patient #8 on axial post-contrast T1-weighted (**N**), apparent diffusion coefficient map (**O**) and sagittal unenhanced CT (**P**) images, showing a partially calcified mass, with low contrast enhancement and strong diffusion restriction that developed from the tectal region through the tentorial incisure

with the *MN1::PATZ1* fusion. A reticulin fibre network was absent in all tumors, outside the vessels, particularly in the spindle cell component. Microcalcifications were observed in 4/12 tumors. Six samples presented microcystic formations, bordered by tumor cells. An adipocytic metaplasia was present in 5/12 tumors (Fig. 2J). When microvascular proliferation was present (4/12 cases), it was associated with the glial multinucleated component. Necrosis (without palisades) was present in two tumors and was always associated to microvascular proliferation and elevated mitotic index. Mitotic and proliferative indexes were variable (median of 4 mitoses/10 high-power fields representing 3.2 mm^2; and median proliferative index of 4%) (Fig. 2K-L), when present, the components were more elevated in the spindle cell pattern. For tumors who recurred, and when histology was available, the histopathological features between the different surgeries were identical. Using NGS analysis, no recurrent genetic alteration was found in the cohort.

Evidence of a glioneuronal differentiation in CNS tumors, PATZ1-fused

The oligodendroglial-like component presented variation in nuclear size and occasional intranuclear inclusions (present in all cases) (Fig. 3A). Perivascular lymphocytic infiltrates were conspicuous in four tumors (#4, 6,

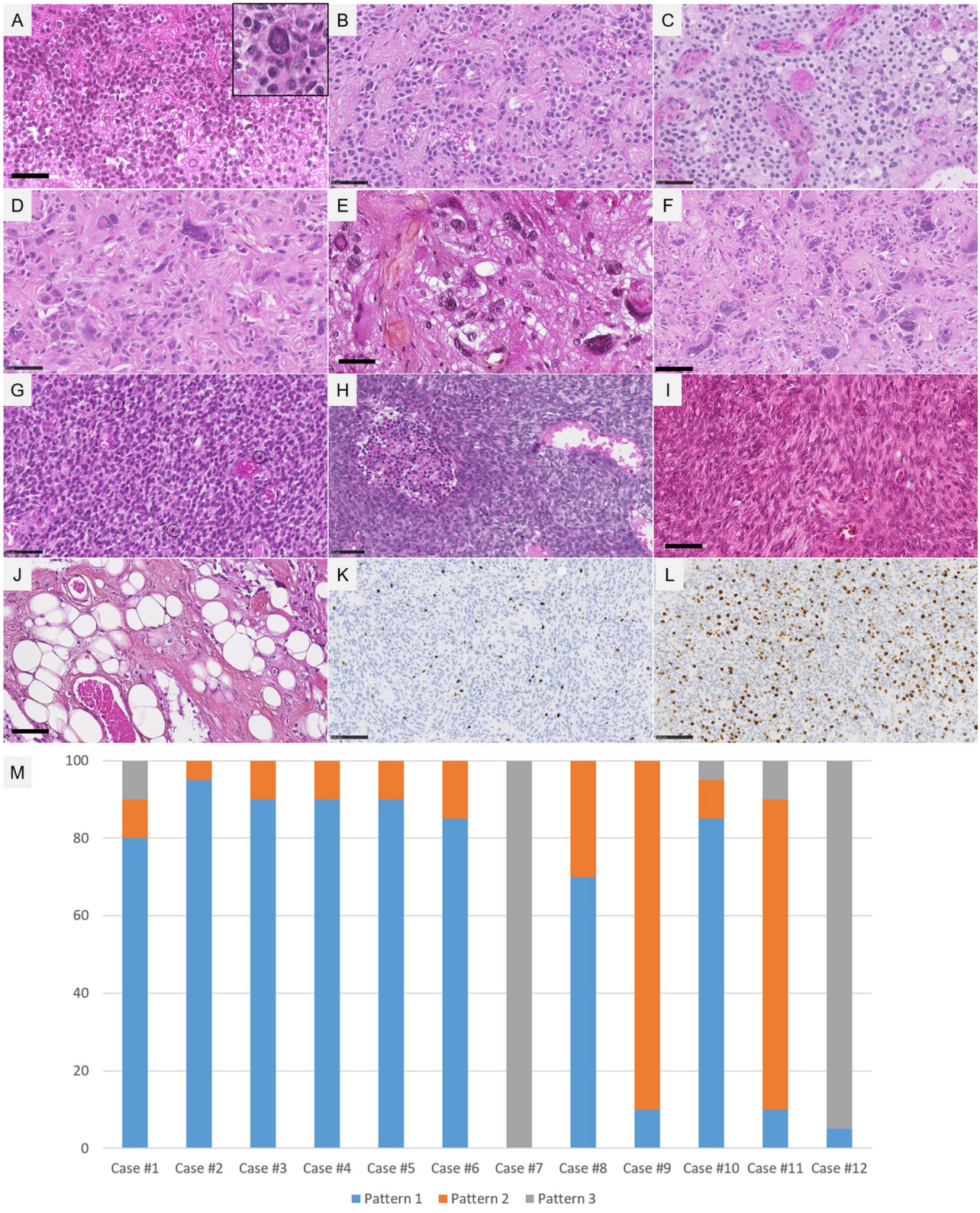

Fig. 2 Main morphological patterns of neuroepithelial tumors, *PATZ1*-fused. **A-C** A glial pattern composed of oligodendroglial-cells intermingled with a dense vascular network of hyalinized vessels (HPS, magnification x400). **D-F** A glial pattern composed of polymorphous and multinucleated cells with intranuclear inclusions (HPS, magnification x400). **G-I** A spindle cell pattern (HPS, magnification x400). **J** The adipocytic metaplasia (HPS, magnification x400). **K-L** A variable Ki67 labeling index (magnification x400). **M** Percentage of areas with the different morphological patterns: pattern 1 (the glial pattern composed of oligodendroglial-cells intermingled with a dense vascular network made of hyalinized vessels), pattern 2 (the glial pattern composed of polymorphous and multinucleated cells), and pattern 3 (the spindle cell component). Black scale bars represent 50 µm. HPS: Hematoxylin Phloxin Saffron

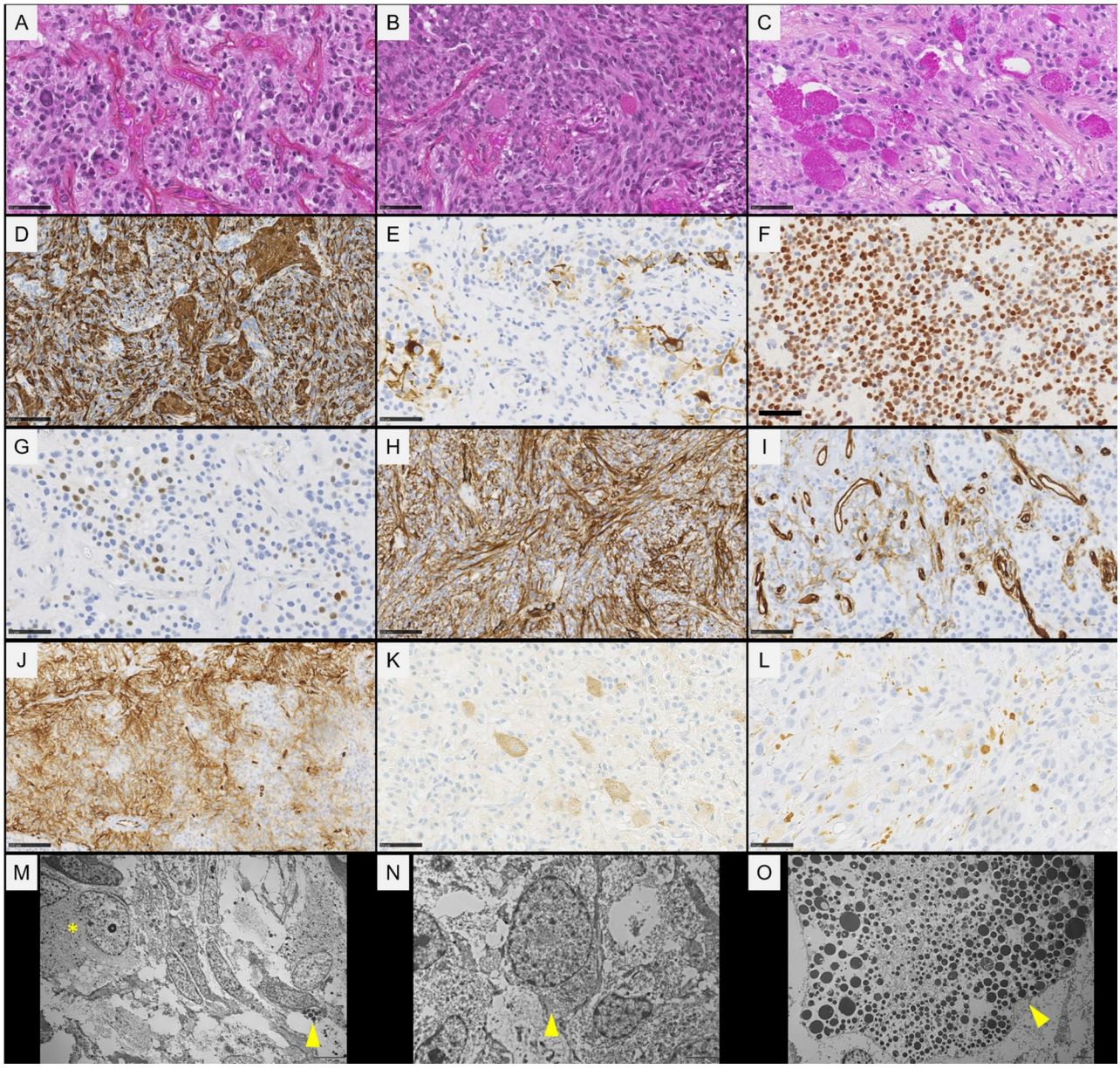

Fig. 3 Morphological, immunophenotypical and ultrastructural findings of glioneuronal differentiation in neuroepithelial tumors, *PATZ1*-fused. **A** Oligodendroglial cells and intranuclear inclusions (HPS, magnification x400, insert HPS, magnification x400). **B-C** Tumor cells with numerous eosinophilic granular bodies (HPS, magnification x400). **D-E** Variable expression of GFAP, moderate to diffuse (HPS, magnification x400). **F-G** Constant but variable expression of OLIG2 by tumor cells (magnification x400). **H-J** Constant extravascular immunopositivity for CD34 in a stellar and cellular manner (magnification x400). **K** Immunoexpression of synaptophysin by a subset of tumor cells (magnification x400). **L** Immunopositivity for chromogranin A in some tumor cells (magnification x400). **M** An astrocytic-like cell with intermediate filaments (asterisk) and dense core granules (neuronal cell) (arrowhead). **N** An oligodendroglial-like cell (arrowhead). **O** A neuronal cell with dense core granules (arrowhead). Black scale bars represent 50 µm. HPS: Hematoxylin Phloxin Saffron

10, and 11). Eosinophilic granular bodies were encountered in five samples (#1, 3, 9, 10, and 11) (Fig. 3B-C). No Rosenthal fibres or dysmorphic neuronal/ganglions were observed.

All specimens exhibited an expression of glial markers (GFAP and OLIG2) with a variable distribution (Fig. 3D-G). All cases except one exhibited an extravascular immunopositivity for CD34 (Fig. 3H-J). This staining was cellular with a membranous reinforcement. No staining was present in the adjacent brain parenchyma. Seven tumors stained for neuronal markers (but three cases were not tested for markers other than synaptophysin) (Fig. 3K-L). Among them, only one sample presented a dot-like immunopositivity for synaptophysin. The spindle cell component also exhibited the expression of glioneuronal markers (focal immunoreactivity for GFAP, OLIG2,

synaptophysin) and CD34. No epithelial or myogenic markers were expressed.

Ultrastructural analyses were available for five cases (samples #1, 2, 3, 4, and 6). All tumors showed ribosomal rosettes, dense core granules, intermediate filaments, indented nuclei, and dilated endoplasmic reticulum, reminiscent of glial and neuronal differentiations (Fig. 3M-O). There were no cilia, microvilli or collagen fibres. In comparison, ultrastructural analyses revealed that sarcomas, *PATZ1*-fused did not show any dense core granules, but presented numerous collagen fibres ($n = 3$).

CNS tumors with PATZ1 fusions cluster in a unique cluster

According to the DNA methylation-based classification of the Heidelberg Brain Tumor Classifier (version 12.8), 11/12 tumors were classifiable as NET-*PATZ1* (eight of them with a calibrated score > 0.9, the last tumor presented a score of 0.68 for the MC of NET-*PATZ1*). A t-SNE analysis was performed to compare the genome-wide DNA methylation profiles of our cases with notably the different methylation classes of glial, glioneuronal, ependymal tumors and astroblastoma-*MN1* in the CNS reference cohort [6]. All cases clustered within the NET-*PATZ1* methylation class.

GATA2 overexpression is sensitive and specific for the detection of CNS tumors, PATZ1-fused

GATA2 was expressed in 6/9 tested CNS tumors with *PATZ1* fusions (Fig. 4A-C). The staining was nuclear and diffuse, with a moderate to strong intensity, and was observed in the different histopathological patterns. We did not observe any expression in sarcomas-*PATZ1* and 112 epigenetically proven tumors constituting potential differential diagnoses: supratentorial ependymomas, *ZFTA*-fused ($n = 30$), gangliogliomas ($n = 15$), pleomorphic xanthoastrocytomas grade 3 ($n = 15$), infant-type hemispheric gliomas ($n = 6$), desmoplastic infantile gangliogliomas/astrocytomas ($n = 10$), meningiomas ($n = 30$),

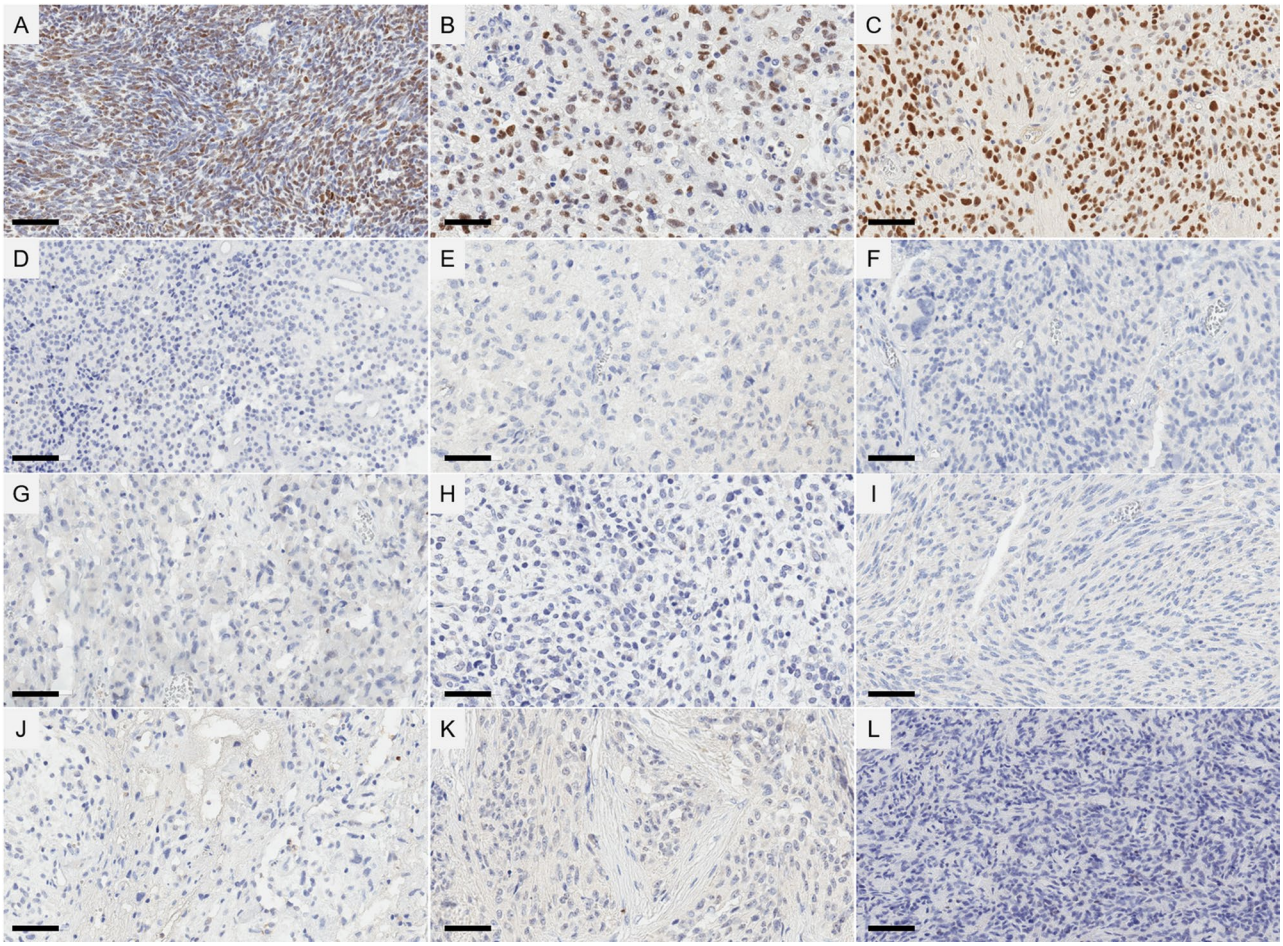

Fig. 4 GATA2 immunoexpression illustrated in various tumor types. **A-C** Diffuse nuclear expression of GATA2 in neuroepithelial tumor-*PATZ1*. No expression in potential differential diagnoses (**D** supratentorial ependymoma, *ZFTA*-fused, **E** ganglioglioma, **F** pleomorphic xanthoastrocytoma, **G** infant-type hemispheric glioma, **H** desmoplastic infantile ganglioglioma, **I** meningioma, **J** intracranial mesenchymal tumor, FET::CREB-fused, **K-L** sarcomas-*PATZ1*). Black scale bars represent 50 µm

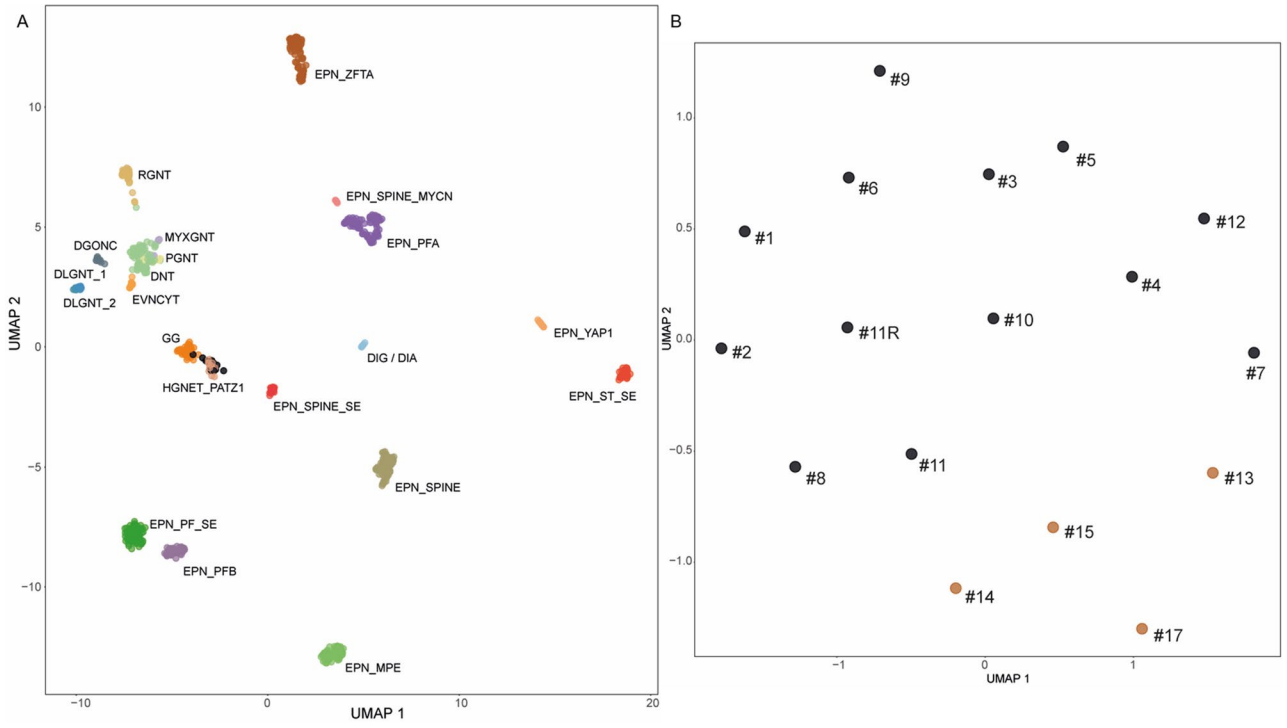

Fig. 5 DNA methylation-based t-distributed stochastic neighbor embedding distribution (**A**, and **B** focused on tumors with *PATZ1* fusions). **A** Our tumors (NET-*PATZ1*: black spots and sarcomas-*PATZ1*: brown spots) were compared to reference samples from the Heidelberg cohort belonging to the DGONC ($n=15$), DIG / DIA ($n=12$), DLGNT_1 ($n=8$), DLGNT_2 ($n=10$), DNT ($n=40$), EPN_MPE ($n=15$), EPN-PFA ($n=91$), EPN_PFB ($n=23$), EPN_PF_SE ($n=12$), EPN_SPINE ($n=21$), EPN_SPINE_MYCN ($n=10$), EPN_ST_SE ($n=12$), EPN_YAP1 ($n=11$), EPN_ZFTA ($n=70$), EVNCYT ($n=15$), GG ($n=22$), HGNET_PATZ1 ($n=40$), MYXGNT ($n=22$), PGNT ($n=12$), and RGNT ($n=14$) methylation classes. The cases in this study were in close proximity to the HGNET_PATZ1 subgroup. In a more focused t-SNE analysis of the samples (**B**), NET-*PATZ1* (black dots) were distinct from sarcomas-*PATZ1* (orange dots)

and intracranial mesenchymal tumors, FET::CREB-fused ($n=6$) (Fig. 4D-J).

CNS tumors are different from sarcomas, PATZ1-fused

The five sarcomas having a *PATZ1* fusion concerned middle-aged adults (ranging from 41 to 57 years of age) (see supplementary Tables 1 and Fig. 1 for details). The tumors were located in the deep soft tissue of the paraventral and chest regions. Histopathologically, they were monomorphous and composed of spindle cells with some microcystic formations. They did not present multinucleated cells, oligodendroglial-like cells, pseudorosettes, intranuclear inclusions or eosinophilic granular bodies. Hyalinized vessels were present in two samples. One tumor presented a myogenic differentiation, without adipocytic metaplasia. Using immunohistochemistry, they did not express neuronal markers or OLIG2, but some focally expressed GFAP. Moreover, sarcomas-*PATZ1* did not express GATA2 (Fig. 4K-L). Argentic impregnation showed an abundant network of reticulin fibres. Ultrastructural analyses of three sarcomas-*PATZ1* failed to identify any glial or neuronal cells. They did not present a dense core, intermediate filaments or eosinophilic granular bodies, but they presented collagen fibres. Genetic studies showed that these sarcomas only exhibited a *EWSR1::PATZ1* fusion. The tumors were not classifiable using the Heidelberg Brain Tumor (v12.8) and sarcoma (v12.2) or Bethesda (v2.0) Classifiers. T-SNE analysis (Fig. 5) showed that sarcomas-*PATZ1* clustered in the vicinity of NET-*PATZ1* but were distinct.

Discussion

Recently, DNA-methylation profiling revealed a novel MC, that has not yet been included as a provisional tumor type in the current WHO classification, the NET-*PATZ1* ($n=79$) [1, 5–20]. The literature, including our cases, has shown that NET-*PATZ1* mainly affect children (71% of patients are younger than 18 years of age, with a median age of 12 years-old), without gender predilection. They are mostly supratentorial (cortical or periventricular) (88%, 68/77), but rare specimens have been reported in the posterior fossa [1, 14] or the spine [1, 16]. Imaging features (from 6 of our series and 19 in the literature) are variable, resembling supratentorial ependymomas (large enhanced tissular masses with cystic content), embryonal tumors or astroblastomas (tissular masses with strong diffusion restriction) [19]. Histopathologically, the tumors described here are in line with the findings in the literature, showing a variety of morphological patterns (glial with oligodendroglial-cells associated with

numerous anastomosing hyalinized vessels, glioneuronal with polymorphous cells, or spindle cells), with an intra- and intertumoral heterogeneity. Herein, we illustrate that, despite this heterogeneity, CNS tumors with *PATZ1* fusions exhibit immunohistochemical (with the expression of glial and neuronal markers, and CD34 immunopositivity) and ultrastructural (ribosomal rosettes, dense core granules, intermediate filaments, indented nuclei, dilated reticulum endoplasmic, glial and neuronal cells) features of a glioneuronal differentiation. These results are in concordance with the results from transcriptomic analyses showing that this tumor type overexpresses neuronal development genes such as *PAX2*, *IGF2* and *GATA2* [1]. Due to this overexpression, we evidenced that the immunoexpression of the protein GATA2 is highly specific to the NET-*PATZ1* diagnosis (6/9 tested tumors with a diffuse and strong immunopositivity) but more importantly, none of the numerous tumoral mimickers expressed GATA2 ($n = 112$). However, it is not perfectly sensitive. Because the current study was multicentric and retrospective, the immunonegativity of the three remaining CNS tumors, *PATZ1*-fused may be due to preanalytical conditions. Further large cohorts with differential diagnoses are needed to confirm if GATA2 immunostaining may help neuropathologists detect this entity. In the CNS, *PATZ1* may be fused with the *EWSR1* (36/59 tumors) or *MN1* (23/59 tumors) genes [1, 5–9, 11–20]. In this study, we showed that no specific correlation exists between the morphological pattern and fusion type, but specimens exhibiting only a spindle cell component are always associated with an *EWSR1::PATZ1* fusion [6].

The adipocytic metaplasia, observed in 5/12 CNS tumors with *PATZ1* fusions, is a rare histopathological feature that can be found in glioneuronal tumors (except cerebellar liponeurocytoma) [21], and may alert neuropathologists to this diagnosis when found in the supratentorial location.

The current study also supports the argument that CNS tumors with *PATZ1* fusions and sarcomas-*PATZ1* are distinct. Indeed, despite a multiphenotypic immunoprofile, the sarcomas do not present ultrastructural features of a glioneuronal origin, but show a well-developed reticulin network (using silver impregnation) and collagen fibres on ultrastructural analyses. Histopathologically, they are monomorphous, composed of small round or spindled cells, and may express markers of myogenic and epithelial lineages. Moreover, sarcomas-*PATZ1* have not been reported with a *MN1::PATZ1* fusion and they do not overexpress the GATA2 protein. Herein, we also show that sarcomas, *PATZ1* do not cluster with NET-*PATZ1* in terms of DNA-methylation profiling.

In accordance with a potential glioneuronal origin, and despite the presence of "aggressive" histological findings (a subset of them being described with a high mitotic index or necrosis) [1, 8, 11, 15, 18], CNS tumors with *PATZ1* fusions seem to be associated with a good prognosis (19/55 local recurrences reported after a subtotal resection, and only 2/56 patients were deceased from tumor progression at the end of follow-up) [1, 5, 8–11, 13–15, 18, 19].

To conclude, the current work shows that CNS tumors *PATZ1*-fused have a glioneuronal differentiation and are characterized by a clinical phenotype (pediatric circumscribed supratentorial tumors with a favorable prognosis), and a unique methylation class. Morphologically, these polymorphous tumors show recurrent histopathological patterns, and an unusual spindle component for glioneuronal tumors. Immunophenotypically, both the GATA2 and CD34 expression may help neuropathologists suggest this challenging diagnosis.

Abbreviations

DGONC	Diffuse glioneuronal tumor with oligodendroglioma-like features and nuclear clusters
DIG / DIA	Desmoplastic infantile ganglioglioma/astrocytoma
DLGNT	Diffuse glioneuronal tumor
DNT	Dysembryoplastic neuroepithelial tumor
EPN	Ependymoma
EVNCYT	Extraventricular neurocytoma
GG	Ganglioglioma
HGNET	High-grade neuroepithelial tumor
MPE	Myxopapillary ependymoma
MYXGNT	Myxoid glioneuronal tumor
PF	Posterior fossa
PGNT	Papillary glioneuronal tumor
RGNT	Rosette-forming glioneuronal tumor
SE	Subependymoma;
ST	Supratentorial

Supplementary Information

The online version contains supplementary material available at https://doi.org/10.1186/s40478-025-02037-5.

Supplementary Material 1

Supplementary Material 2

Supplementary Material 3

Acknowledgements

We would like to thank the laboratory technicians at GHU Paris Neuro Sainte-Anne for their assistance, and the RENOCLIP-LOC. The RENOCLIP-LOC is the clinico-pathologic network that is instrumental in the central histopathologic review supported by the Institut National du Cancer (INCa).

Author contributions

ATE, VDR, NB, KB and TB compiled the MRI and clinical records; ATE, AM, MD, AS, CN, FLL, CB, AF, AR, FM, EUC and PV conducted the neuropathological examinations; ATE, PS, YN and EUC conducted the molecular studies; PV, LH and ATE drafted the manuscript; all authors reviewed the manuscript.

Funding

The authors have received no external funding for this study.

Data availability

No datasets were generated or analysed during the current study.

Declarations

Ethics approval and consent to participate
This study was approved by GHU Paris Psychiatry and Neurosciences, Sainte-Anne Hospital's local ethic committee.

Consent for publication
The patient signed informed consent forms before treatment was started.

Competing interests
The authors declare no competing interests.

Author details
[1]Department of Neuropathology, GHU Paris-Psychiatrie et Neurosciences, Sainte-Anne Hospital, Paris, France
[2]Institut de Psychiatrie et Neurosciences de Paris (IPNP), UMR S1266, INSERM, IMA-BRAIN, Paris, France
[3]Université de Paris, Paris, France
[4]Pediatric Radiology Department, AP-HP, Hôpital Universitaire Necker-Enfants Malades, Paris F-75015, France
[5]Université de Paris, INSERM ERL UA10, INSERM U1163, Institut Imagine, Paris F-75015, France
[6]Department of Neuropathology, Institute of Pathology, University Hospital Heidelberg, Heidelberg, Germany
[7]Clinical Cooperation Unit Neuropathology, German Consortium for Translational Cancer Research (DKTK), German Cancer Research Center DKFZ, Heidelberg, Germany
[8]Department of Pathology, Dupuytren University Hospital, Limoges, France
[9]Department of Pathology, Toulouse University Hospital, Toulouse, France
[10]INSERM U1037, Cancer Research Center of Toulouse (CRCT), Toulouse, France
[11]Université Paul Sabatier, Toulouse III, Toulouse, France
[12]Department of Pathology, Gustave Roussy Institute, Villejuif, France
[13]Department of Biopathology, Institut Bergonié, Bordeaux, France
[14]Université de Bordeaux, Talence, France
[15]INSERM U1218, ACTION, Institut Bergonié, Bordeaux, France
[16]Inst Neurophysiopathol, and APHM, Department of Anatomopathology and Neuropathology, Aix-Marseille Univ, CNRS, INP, La Timone Hospital, Marseille 13385, France
[17]Department of Pathology, Angers Hospital, Angers, France
[18]Université d'Angers, Inserm UMR 1307, CNRS UMR 6075, Nantes Université, CRCI2NA, Angers F-49000, France
[19]Department of Pathology, Rouen Hospital, Rouen, France
[20]Department of Pediatric Neurosurgery, APHP, Necker Hospital, Université Paris Descartes, Sorbonne Paris Cité, Paris, France
[21]Department of Neuropathology, GHU Paris-Psychiatrie et Neurosciences, Sainte-Anne Hospital, 1, rue Cabanis, Paris 75014, France

Received: 7 April 2025 / Accepted: 10 May 2025
Published online: 24 May 2025

References
1. Alhalabi KT, Stichel D, Sievers P, Peterziel H, Sommerkamp AC, Sturm D, Wittmann A, Sill M, Jäger N, Beck P, Pajtler KW, Snuderl M, Jour G, Delorenzo M, Martin AM, Levy A, Dalvi N, Hansford JR, Gottardo NG, Uro-Coste E, Maurage C-A, Godfraind C, Vandenbos F, Pietsch T, Kramm C, Filippidou M, Kattamis A, Jones C, Øra I, Mikkelsen TS, Zapotocky M, Sumerauer D, Scheie D, McCabe M, Wesseling P, Tops BBJ, Kranendonk MEG, Karajannis MA, Bouvier N, Papaemmanuil E, Dohmen H, Acker T, von Hoff K, Schmid S, Miele E, Filipski K, Kitanovski L, Krskova L, Gojo J, Haberler C, Alvaro F, Ecker J, Selt F, Milde T, Witt O, Oehme I, Kool M, von Deimling A, Korshunov A, Pfister SM, Sahm F, Jones DTW (2021) PATZ1 fusions define a novel molecularly distinct neuroepithelial tumor entity with a broad histological spectrum. Acta Neuropathol (Berl) 142:841–857. https://doi.org/10.1007/s00401-021-02354-8
2. Al-Obaidy KI, Bridge JA, Cheng L, Sumegi J, Reuter VE, Benayed R, Hameed M, Williamson SR, Hes O, Alruwaii FI, Segal JP, Wanjari P, Idrees MT, Nassiri M, Eble JN, Grignon DJ (2021) EWSR1-PATZ1 fusion renal cell carcinoma: a recurrent gene fusion characterizing thyroid-like follicular renal cell carcinoma. Mod Pathol Off J U S Can Acad Pathol Inc 34:1921–1934. https://doi.org/10.1038/s41379-021-00833-7
3. Watson S, Perrin V, Guillemot D, Reynaud S, Coindre J-M, Karanian M, Guinebretière J-M, Freneaux P, Le Loarer F, Bouvet M, Galmiche-Rolland L, Larousserie F, Longchampt E, Ranchere-Vince D, Pierron G, Delattre O, Tirode F (2018) Transcriptomic definition of molecular subgroups of small round cell sarcomas. J Pathol 245:29–40. https://doi.org/10.1002/path.5053
4. Fontaine A, Basset L, Milin S, Argentin J, Uro-Coste E, Rousseau A (2025) [Neuroepithelial tumor with PATZ1 fusion - case report and focus on an ill-defined entity]. Ann Pathol 45:92–96. https://doi.org/10.1016/j.annpat.2024.01.002
5. Siegfried A, Rousseau A, Maurage C-A, Pericart S, Nicaise Y, Escudie F, Grand D, Delrieu A, Gomez-Brouchet A, Le Guellec S, Franchet C, Boetto S, Vinchon M, Sol J-C, Roux F-E, Rigau V, Bertozzi A-I, Jones DTW, Figarella-Branger D, Uro-Coste E (2019) EWSR1-PATZ1 gene fusion May define a new glioneuronal tumor entity. Brain Pathol Zurich Switz 29:53–62. https://doi.org/10.1111/bpa.12619
6. Rossi S, Barresi S, Colafati GS, Genovese S, Tancredi C, Costabile V, Patrizi S, Giovannoni I, Asioli S, Poliani PL, Gardiman MP, Cardoni A, Del Baldo G, Antonelli M, Gianno F, Piccirilli E, Catino G, Martucci L, Quacquarini D, Toni F, Melchionda F, Viscardi E, Zucchelli M, Dal Pos S, Gatti E, Liserre R, Schiavello E, Diomedi-Camassei F, Carai A, Mastronuzzi A, Gessi M, Giannini C, Novelli A, Onetti Muda A, Miele E, Alesi V, Alaggio R (2024) PATZ1-Rearranged tumors of the central nervous system: characterization of a pediatric series of seven cases. Mod Pathol Off J U S Can Acad Pathol Inc 37:100387. https://doi.org/10.1016/j.modpat.2023.100387
7. Bridge JA, Sumegi J, Druta M, Bui MM, Henderson-Jackson E, Linos K, Baker M, Walko CM, Millis S, Brohl AS (2019) Clinical, pathological, and genomic features of EWSR1-PATZ1 fusion sarcoma. Mod Pathol Off J U S Can Acad Pathol Inc 32:1593–1604. https://doi.org/10.1038/s41379-019-0301-1
8. Burel-Vandenbos F, Pierron G, Thomas C, Reynaud S, Gregoire V, Duhil de Benaze G, Croze S, Chivoret N, Honavar M, Figarella-Branger D, Maurage C-A, Pedeutour F, Hasselblatt M, Godfraind C (2020) A polyphenotypic malignant paediatric brain tumour presenting a MN1-PATZ1 fusion, no epigenetic similarities with CNS High-Grade neuroepithelial tumour with MN1 alteration (CNS HGNET-MN1) and related to PATZ1-fused sarcomas. Neuropathol Appl Neurobiol 46:506–509. https://doi.org/10.1111/nan.12626
9. Chadda KR, Holland K, Scoffings D, Dean A, Pickles JC, Behjati S, Jacques TS, Trotman J, Tarpey P, Allinson K, Murray MJ, Genomics England Research Consortium (2021) A rare case of paediatric astroblastoma with concomitant MN1-GTSE1 and EWSR1-PATZ1 gene fusions altering management. Neuropathol Appl Neurobiol. https://doi.org/10.1111/nan.12701
10. Di Ruscio V, Carai A, Del Baldo G, Vinci M, Cacchione A, Miele E, Rossi S, Antonelli M, Barresi S, Caulo M, Colafati GS, Mastronuzzi A (2022) Molecular landscape in infant High-Grade gliomas: A single center experience. Diagn Basel Switz 12:372. https://doi.org/10.3390/diagnostics12020372
11. Ene A, Di J, Neltner JH, Pittman T, Arnold SM, Kolesar JM, Villano JL, Bachert SE, Allison DB (2023) Case report: A unique presentation of a high-grade neuroepithelial tumor with EWSR1::PATZ1 fusion with diagnostic, molecular, and therapeutic insights. Front Oncol 13:1094274. https://doi.org/10.3389/fonc.2023.1094274
12. Johnson A, Severson E, Gay L, Vergilio J, Elvin J, Suh J, Daniel S, Covert M, Frampton GM, Hsu S, Lesser GJ, Stogner-Underwood K, Mott RT, Rush SZ, Stanke JJ, Dahiya S, Sun J, Reddy P, Chalmers ZR, Erlich R, Chudnovsky Y, Fabrizio D, Schrock AB, Ali S, Miller V, Stephens PJ, Ross J, Crawford JR, Ramkissoon SH (2017) Comprehensive genomic profiling of 282 pediatric Low- and High-Grade gliomas reveals genomic drivers, tumor mutational burden, and hypermutation signatures. Oncologist 22:1478–1490. https://doi.org/10.1634/theoncologist.2017-0242
13. Kim H, Lee K, Phi JH, Paek SH, Yun H, Choi SH, Park S-H (2023) Neuroepithelial tumor with EWSR1::PATZ1 fusion: A literature review. J Neuropathol Exp Neurol 82:934–947. https://doi.org/10.1093/jnen/nlad076
14. Kumar N, Malicki D, Levy M, Crawford JR (2023) Rare posterior fossa EWSR1-PATZ1 gene fusion glioneuronal tumour-mimicking ependymoma in an adolescent successfully treated with surgery alone. BMJ Case Rep 16:e256055. https://doi.org/10.1136/bcr-2023-256055
15. Lopez-Nunez O, Cafferata B, Santi M, Ranganathan S, Pearce TM, Kulich SM, Bailey KM, Broniscer A, Rossi S, Zin A, Nasrallah MP, Li MM, Zhong Y, Miele E, Alaggio R, Surrey LF (2021) The spectrum of rare central nervous system (CNS) tumors with EWSR1-non-ETS fusions: experience from three pediatric institutions with review of the literature. Brain Pathol Zurich Switz 31:70–83. https://doi.org/10.1111/bpa.12900

16. Pei J, Zhao X, Patchefsky AS, Flieder DB, Talarchek JN, Testa JR, Wei S (2019) Clinical application of RNA sequencing in sarcoma diagnosis: an institutional experience. Med (Baltim) 98:e16031. https://doi.org/10.1097/MD.0000000000016031
17. Qaddoumi I, Orisme W, Wen J, Santiago T, Gupta K, Dalton JD, Tang B, Haupfear K, Punchihewa C, Easton J, Mulder H, Boggs K, Shao Y, Rusch M, Becksfort J, Gupta P, Wang S, Lee RP, Brat D, Peter Collins V, Dahiya S, George D, Konomos W, Kurian KM, McFadden K, Serafini LN, Nickols H, Perry A, Shurtleff S, Gajjar A, Boop FA, Klimo PD, Mardis ER, Wilson RK, Baker SJ, Zhang J, Wu G, Downing JR, Tatevossian RG, Ellison DW (2016) Genetic alterations in uncommon low-grade neuroepithelial tumors: BRAF, FGFR1, and MYB mutations occur at high frequency and align with morphology. Acta Neuropathol (Berl) 131:833–845. https://doi.org/10.1007/s00401-016-1539-z
18. Rossi S, Barresi S, Giovannoni I, Alesi V, Ciolfi A, Colafati GS, Diomedi-Camassei F, Miele E, Cacchione A, Quacquarini D, Carai A, Tartaglia M, Giannini C, Giangaspero F, Mastronuzzi A, Alaggio R (2020) Expanding the spectrum of EWSR1-PATZ1 rearranged CNS tumors: an infantile case with leptomeningeal dissemination. Brain Pathol Zurich Switz e12934. https://doi.org/10.1111/bpa.12934
19. Vanmarcke C, Marcelis L, Bempt IV, Sciot R, Devos J (2024) The imaging appearance of EWSR1::PATZ1 gene fusion central nervous system tumors. J Belg Soc Radiol 108:107. https://doi.org/10.5334/jbsr.3431
20. Zschernack V, Jünger ST, Mynarek M, Rutkowski S, Garre ML, Ebinger M, Neu M, Faber J, Erdlenbruch B, Claviez A, Bielack S, Brozou T, Frühwald MC, Dörner E, Dreschmann V, Stock A, Solymosi L, Hench J, Frank S, Vokuhl C, Waha A, Andreiuolo F, Pietsch T (2021) Supratentorial ependymoma in childhood: more than just RELA or YAP. Acta Neuropathol (Berl) 141:455–466. https://doi.org/10.1007/s00401-020-02260-5
21. Broggi G, Salzano S, Mazzucchelli M, Rosano GN, Magro G, Caltabiano R, Barresi V (2025) Cerebellar liponeurocytoma: an updated comprehensive review of clinicopathologic, immunohistochemical, and molecular features of an unusual but distinct tumor. Clin Neuropathol. https://doi.org/10.5414/NP301660

Publisher's note